

1 **Online supplementary materials and methods**

2 **Study design**

3 The overall objectives were to explore the pathogenic mechanisms of RASFs through elucidating the genetic
4 contribution to molecular regulatory networks under inflammatory condition. First, we quantified mRNA
5 expression by RNA sequencing and compared transcriptome of SFs between the 10 conditions (i.e., non-stimulated,
6 IFN- α , IFN- γ , TNF- α , IL-1 β , IL-6/sIL-6R, IL-17, TGF- β 1, IL-18 or 8-mix) and the diseases (i.e., RA, OA). We
7 next performed cis-eQTL analysis to evaluate the effect of genetic variants on gene expressions in stimulated SFs
8 and five major immune cell subsets (CD4⁺ T cells, CD8⁺ T cells, B cells, NK cells, monocytes) from the same
9 patient. In addition, we examined candidate causal genes among RA risk loci in SFs. Focusing on eQTL variants in
10 LD with GWAS top-associated loci, we assessed the biological role of the CD40-CD40L pathway in SFs by
11 transcriptomic analysis of RASFs stimulated with a 2-trimer form of the CD40 ligand and IFN- γ as a representative
12 example. Next, in order to elucidate the link between RA genetic risk and transcriptomic and epigenomic
13 perturbations of stimulated SFs, we performed a gene-set enrichment analysis with RA-associated genetic loci and
14 assessed the enrichment of GWAS top-associated loci in regulatory regions (SEs or TEs) identified with ChIP
15 sequencing. Furthermore, we combined the 3D genome architectures (chromatin loops detected by Hi-C analysis),
16 the position of SEs, promoter regions (defined with H3K4me3 ChIP sequencing analysis) in SFs under 3 different
17 conditions: non-stimulated, TNF- α or the 8-mix. To reveal candidate modulators crucial for SE formation,
18 especially in the 8-mix, we integrated motif analysis to focus on SE-contacted TFs that were also enriched in 8-mix
19 SEs and compared them with TEs or stimulated SEs. Finally, the promising pathogenic TFs (i.e., MTF1, RUNX1)

20 in RASFs were silenced with siRNAs to validate transcriptomic effects, and the impact of MTF1 inhibitor was
21 assessed by *in vitro* and *in vivo* assay.

22

23 **Patient and public involvement**

24 Patients and/or the public were not involved in the design, or conduct, or reporting, or dissemination plans of this
25 research.

26

27 **Human participants and sample collection**

28 Synovial tissues were obtained from RA and OA patients (n = 30 each) undergoing joint replacement surgery at the
29 University of Tokyo Hospital, Japan. RA patients fulfilled the 2010 ACR/EULAR (American College of
30 Rheumatology/European League Against Rheumatism) criteria for the classification of RA.[1] Patient
31 characteristics are summarized in online supplementary table 5. This study was approved by the Ethics Committees
32 of the University of Tokyo (G3582), RIKEN and the indicated medical institutions. Written informed consent was
33 obtained from each subject in accordance with the Declaration of Helsinki. Fresh synovial tissues were minced and
34 digested with 0.1% collagenase (Worthington) at 37°C, in 5% CO₂ for 1.5 h and SFs were cultured in Dulbecco's
35 modified Eagle's medium (DMEM; SIGMA) supplemented with 10% fetal bovine serum (FBS; BioWest), 100
36 µg/mL L-glutamine, 100 U/mL penicillin, 100 µg/mL streptomycin (all from Invitrogen). SFs from passage 2 or 3
37 were used for RNA sequencing, ChIP sequencing, Hi-C and functional studies after removal of macrophages by
38 magnetic separation with CD14 microbeads (Miltenyi Biotec). The purity of SFs was tested by flow cytometry

39 analysis (MoFlo XDP; Beckman Coulter). SFs were stained with CD14⁻, Thy-1 (CD90)-specific monoclonal
40 antibodies (clone IDs: M5E2, 5E10, respectively, all from BioLegend). Most cells (>99%) had the surface marker
41 for fibroblasts (Thy-1) but not CD14.

42 We collected peripheral blood from the same patients. PBMCs were isolated using Ficoll-Paque density gradient
43 centrifugation followed by staining with CD3⁻, CD4⁻, CD8⁻, CD14⁻, CD19⁻ and CD56-specific monoclonal
44 antibodies (clone IDs: UCHT1, OKT4, RPA-T8, M5E2, HIB19 and HCD56, respectively, all from BioLegend).

45 Five immune cell populations were sorted by flow cytometry (MoFlo XDP; Beckman Coulter) using the following
46 gating strategy: CD4⁺ T cells: CD3⁺CD4⁺CD8⁻CD19⁻; CD8⁺ T cells: CD3⁺CD4⁻CD8⁺CD19⁻; B cells: CD3⁻CD19⁺;
47 NK cells: CD3⁻CD14⁻CD19⁻CD56⁺; and monocytes: CD3⁻CD14⁺CD19⁻. There were 3×10^5 cells in each
48 population.

49

50 RNA sequencing

51 Purified SFs (2×10^4 cells/well) were seeded with DMEM (10% FBS, 100 µg/mL L-glutamine, 100 U/mL
52 penicillin, 100 µg/mL streptomycin) into a 24-well flat-bottom plate (Corning) and incubated at 37°C, in 5% CO₂.
53 After 12 h, one of the following was added: 100 U/mL IFN-α (HumanZyme), 200 U/mL IFN-γ, 10 ng/mL TNF-α,
54 10 ng/mL IL-1β, 200 ng/mL IL-6/sIL-6R, 10 ng/mL IL-17 (all from PeproTech), 10 ng/mL TGF-β1 (R&D), 100
55 ng/mL IL-18 (MBL). Alternatively, cells were treated with “8-mix” (a mixture of the above 8 cytokines that
56 simulated synergistic inflammation in arthritic joints).

57 These 8 cytokines were selected by a literature search (PubMed) for 1) cytokines mainly secreted by immune cells

58 and involved in pathological phenotype formation of SFs, 2) cytokines mainly secreted by SFs and acting as
59 autocrine, and 3) existing therapeutic targets. The number of papers was greatest in IFN- γ , IFN- α , TNF- α , IL-1 β ,
60 IL-17A, IL-18 and TGF- β 1 for 1), in IL-6 for 2) and in TNF- α , IL-1 β and IL-6 for 3). The cells were stimulated
61 for an additional 24 h at 37°C, in 5% CO₂.

62 Total RNA from SFs and freshly sorted PBMCs was isolated using AllPrep DNA/RNA/miRNA Universal Kit
63 (Qiagen). Libraries for RNA sequencing were prepared using TruSeq Stranded mRNA Library Prep Kit (Illumina).
64 RNA sequencing was carried out on Illumina HiSeq 2500 (read length of 125 bp, paired end).

65

66 **Bioinformatic analysis of RNA sequencing data**

67 RNA sequencing reads were aligned to the human genome assembly hg19/GRCh37 excluding minor haplotypes,
68 random and unknown sequences. Alignment of the reads was performed by STAR (version 2.5.3) (Key resources
69 information) based on the GENCODE v27 (GRCh37 version) annotation. We only utilized reads that were uniquely
70 mapped (corresponding to a mapping quality of 255 for BAM files) and properly paired for further analysis.

71 Gene-level read counts were quantified with HTSeq (version 0.6.0) (Key resources information) based on the
72 GENCODE v27, with strand-specific assay mode and the other default parameters. Transcript-level quantifications
73 were calculated with RSEM (version 1.3.0) (Key resources information).

74 We assessed the quality of each RNA sequencing sample by calculating the mean expression correlation
75 coefficient with other samples with the same stimulatory conditions, equivalent to D statistics as described
76 elsewhere.[2] All samples satisfied more than 10 million uniquely mapped read counts. We excluded samples the D

77 statistics of which were lower than 0.9, resulting in 29 excluded samples (4 non-stimulated, 4 in TNF- α , 3 in IFN- α ,
78 2 in IFN- γ , 6 in IL-1 β , 4 in TGF- β 1, 2 in IL-17, 3 in 8-mix and 1 CD8⁺ T cell). The remaining 856 samples were
79 utilized for the analysis.

80 Differential expression analysis was performed with the edgeR package (Key resources information) with
81 gene-level count data. For each comparison, genes whose expression was less than 10 in more than 90% of samples
82 were excluded. Gender was included as a covariate for all the comparative analyses. RUVseq R package (Key
83 resources information) was utilized for finding hidden factors using 1000 nonvariable genes with conditions as
84 negative control genes and unstimulated samples as negative control samples. Gender and 3 RUV factors were
85 considered covariates in differential expression analysis. Genes with FDR less than 0.05 in the glm1 RT test
86 implemented in edgeR were regarded as differentially expressed genes (DEGs).

87 Gene set enrichment of DEGs to "C2 canonical pathway" gene sets in MSigDB (Key resources information) was
88 analyzed using the clusterProfiler package (Key resources information).

89 MAGMA software (Key resources information) was applied for gene-set analysis of GWAS data. We utilized RA
90 GWAS summary statistics of European ancestry or East Asian ancestry and performed gene set enrichment analysis
91 following the instruction by the authors.[3] Briefly, we carried out "gene analysis" for GWAS summary statistics
92 using the 1000 genomes LD panels (European panel for European GWAS and East Asian panel for East Asian
93 GWAS) and GENCODE v27 gene annotation. Then we carried out "gene-set analysis" using log-fold change of
94 gene expression between conditions as gene covariate and performed enrichment analysis.

95

96 ChIP sequencing

97 Purified SFs (1×10^5 cells/well) were seeded with DMEM (10% FBS, 100 $\mu\text{g/mL}$ L-glutamine, 100 U/mL
98 penicillin, 100 $\mu\text{g/mL}$ streptomycin) into 6-well flat-bottom plates (Corning) and incubated at 37°C, in 5% CO₂.
99 After 12 h, 100 U/mL IFN- α , 200 U/mL IFN- γ , 10 ng/mL TNF- α , 10 ng/mL IL-1 β , 200 ng/mL IL-6/sIL-6R, 10
100 ng/mL IL-17, 10 ng/mL TGF- β 1, 100 ng/mL IL-18 or 8-mix was added. The cells were stimulated for additional 24
101 h at 37°C, in 5% CO₂.

102 Pooled SFs and freshly sorted PBMCs from RA or OA patients (n = 20 each) were cross-linked with 1%
103 formaldehyde for 15 min at room temperature. Chromatin was prepared from pellets of SFs (1×10^7 cells) and
104 PBMCs (2×10^7 cells) using a CHIP-IT High Sensitivity Kit and CHIP-IT PBMC Kit (both from Active Motif),
105 respectively. Sonication was carried out by Covaris S2 (Covaris). The shearing efficiency was analyzed by agarose
106 gel electrophoresis after RNase treatment, reversion of crosslinking and purification of DNA. Sheared chromatin (3
107 μg) was immunoprecipitated using 4 μL of each rabbit polyclonal antibody (H3K4me1, H3K4me3, H3K27ac, all
108 from Active Motif). Sheared chromatin was used as the input DNA. Immunoprecipitated DNA was quantified with
109 the Qubit dsDNA HS Kit (Invitrogen). Libraries for ChIP sequencing were prepared using TruSeq ChIP Library
110 Prep Kit (Illumina) with 5 ng of DNA fragments. DNA size selection (250 - 300 bp) was carried out by BluePippin
111 (Sage Science). ChIP sequencing was carried out on an Illumina HiSeq 2500 (read length of 50 bp, single end).

112

113 Bioinformatics analysis of ChIP sequencing data

114 Sequencing reads from each ChIP sequencing sample were mapped to human genome assembly hg19/GRCh37

115 using Bowtie2 (Key resources information). PCR duplicates were removed, and only uniquely mapped reads were
116 used for peak calling. MACS 2.0 (Key resources information) was used to detect peaks which were enriched in
117 immunoprecipitated samples over the input. Peak calling was performed with narrow peak mode for H3K4me3 and
118 H3K27ac and broad peak mode for H3K4me1.

119 NSC and RSC were calculated by cross-correlation analysis following ENCODE guidelines and samples with
120 NSC less than 1.1 or RSC less than 1 were removed from the analysis.[4] Also, samples with <10 million effective
121 sequence reads were removed. As a result, 4 samples (RA_CD8_H3K27ac, OA_CD8_H3K27ac,
122 OA_IL17_H3K27ac and RA_CD8_H3K4me3) were excluded and the remaining 86 samples were utilized for
123 further analysis.

124 SEs were identified with the Rank Ordering of Super-Enhancers (ROSE) algorithm (Key resources information)
125 based on the H3K27ac ChIP sequencing signal with default parameters.

126 Differentially bound peak analysis for each condition was performed with HOMER software (Key resources
127 information) with fold-enrichment threshold of 2 and Poisson enrichment P value threshold of 0.0001.

128 Motif enrichment analysis was performed with HOMER software. As motifs of some TFs associated with SEs
129 were not included in the HOMER database, we customized motif reference with MotifDb software (Key resources
130 information) for SE associated genes only with *homo sapiens* data.

131

132 **Library construction for Hi-C**

133 Purchased RASFs (n = 7, Articular Engineering) were used to generate an *in situ* Hi-C library as previously

134 described with minor modifications.[5] Briefly, SFs (1×10^5 cells/well) were seeded with DMEM (10% FBS, 100
135 $\mu\text{g/mL}$ L-glutamine, 100 U/mL penicillin, 100 $\mu\text{g/mL}$ streptomycin) into 6-well flat-bottom plates and incubated at
136 37°C , in 5% CO_2 . After 12 h, either 10 ng/mL TNF- α or 8-mix was added, and the cells were stimulated for an
137 additional 24 h at 37°C , in 5% CO_2 . Pooled SFs (2.8×10^6 cells) were cross-linked with 1% formaldehyde for 10
138 min at room temperature. The nuclei were permeabilized, and DNA was digested with 100 units of Mbo I
139 restriction enzyme (NEB). The ends of restriction fragments were labeled with biotinylated nucleotides (dATP;
140 Invitrogen), and proximity ligation was performed. After reversal of crosslinks, ligated DNA was purified and
141 sheared to a length of roughly 400 base pairs with Covaris S2 (Covaris), at which point ligation junctions were
142 pulled down with streptavidin beads (Invitrogen). Sequencing libraries were prepared with a Nextera Mate Pair
143 Sample Preparation Kit (Illumina) and sequenced using a HiSeq series (read length of 150 bp, paired-end read).

144

145 **Bioinformatics analysis of Hi-C data**

146 Sequencing reads from 3 samples were mapped to human genome assembly hg19/GRCh37 using BWA-mem
147 which is implemented in JUICER software (ver 1.8.9) (Key resources information). Loops were called using
148 HiCCUPS software (Key resources information) implemented in JUICER with resolution of 5 kbp, 10 kbp and 25
149 kbp and merged loops were used for downstream analysis.

150

151 **SNP typing and imputation**

152 Genomic DNA from whole blood was isolated using QIAamp DNA Blood Midi Kit (Qiagen). Genotyping was

153 performed using Infinium OmniExpressExome BeadChips (Illumina).

154 Quality control of the genotyping data was performed using PLINK 1.90 (Key resources information), with a SNP
155 call rate > 0.99, HWE < 1×10^{-6} and sample call rate > 0.98. For genome-wide imputation, 595693 post-QC SNPs
156 were pre-phased using SHAPEIT (Key resources information) and imputation was performed using IMPUTE2
157 (Key resources information) with the 1000 Genomes Phase 3 panel as reference. Post-imputation QC was
158 performed using SNPTEST (Key resources information). Genotyped and imputed autosomal SNPs or indels with
159 $MAF \geq 0.05$ were used for cis-eQTL analysis (6124313 variants in total).

160

161 **Cis-eQTL analysis**

162 For cis-eQTL analysis, genes detected in at least half of the samples under at least 1 condition were included. The
163 counts per million (CPM) matrix was normalized between samples using TMM as implemented in edgeR software,
164 normalized across samples using an inverse normal transform and normalized using PEER (Key resources
165 information) with 15 hidden confounders, and the residuals were used for analysis. We used QTLtools (Key
166 resources information) conditional pass for tissue-by-tissue eQTL analysis. In addition, to improve analytical ability,
167 we jointly analyzed the RA and OA samples. We performed a meta-analysis across SFs in various stimulatory
168 conditions and PBMC samples for eQTLs by utilizing Meta-Tissue software (Key resources information), a linear
169 mixed model that allows for heterogeneity in effect sizes across conditions. Cis-eQTL analysis was performed for
170 variants with $MAF \geq 0.05$ within a 1 Mb window around each gene.

171 For each eQTL, we estimated the posterior probability that the effect is shared in each tissue (*m*-value) along with

172 tissue-by-tissue eQTL analysis P value.

173 For comparison of eQTL effect sizes between RA and OA samples, we performed a likelihood ratio test between
174 the 2 nested models using the R anova function (two-sided). The null model, H_0 , and alternative model, H_1 are
175 detailed in the following equations:

$$H_0 : E \approx I + \beta_1 G + \beta_2 D$$

$$H_1 : E \approx I + \beta_1 G + \beta_2 D + \beta_3 D \times G$$

176 where E is the normalized eGene expression, I is the intercept, G is the eVariant genotype, D is the disease term
177 (RA or OA), and β_1 , β_2 and β_3 are the regression coefficients.

178 At first, we tested all of genome-wide significant eQTL variants (2,114,141 variants, $FDR < 0.1$ or m -value $>$
179 0.9) for disease interaction, which resulted in 6 loci achieving genome-wide significance ($FDR < 0.1$, the upper
180 panel of online supplementary figure 2C). Second, when we limited our analyses to genome-wide significant eQTL
181 variants which overlap with histone marks (244,195 variants which overlap with H3K4me3, H3K27ac or
182 H3K4me1 peaks), 8 loci achieved genome-wide significance ($FDR < 0.1$, the middle panel of online supplementary
183 figure 2C). Finally, when we limited our analyses to genome-wide significant eQTL variants which overlap with
184 differential peaks in any of the histone marks between RA and OA (4,087 variants), 12 loci achieved genome-wide
185 significance ($FDR < 0.1$, the lower panel of online supplementary figure 2C). We considered these 12 loci as
186 disease-specific eQTLs.

187

188 **GWAS enrichment analysis**

189 In order to calculate GWAS variant enrichment for epigenomic marks, we prepared 10,000 sets of randomly
190 sampled variants that were matched to GWAS variants for distance from the nearest TSS, minor allele frequency
191 (MAF), gene density and the number of LD variants ($r^2 \geq 0.5$) using SNPSNAP (Key resources information). We
192 counted the number of GWAS variants or randomly selected variants whose LD ($r^2 \geq 0.8$) variants or itself
193 coincided with epigenomic marks. We calculated the empirical P value by comparing the number of GWAS
194 variants that tagged epigenomic marks against the number of randomly selected variants that tagged epigenomic
195 marks. We pruned GWAS variants such that no 2 variants were within 1 Mb of one another, and all GWAS variants
196 within the extended MHC region (25 - 35 Mb on chromosome 6) were removed from the analysis.

197

198 **Population enrichment score**

199 In order to assess the abundance of SF populations reported in the single-cell transcriptome based analysis,[6] we
200 calculated the population enrichment score of each SFs sample. We used “top 20 marker genes for each single-cell
201 RNA sequencing cluster” of 4 SF clusters from the article and calculated the enrichment score of these gene sets
202 using GSVA software (Key resources information) with normalized CPM.

203

204 **cDNA synthesis and qRT-PCR**

205 Purified RASFs (2×10^4 cells/well) were seeded with DMEM (10% FBS, 100 $\mu\text{g/mL}$ L-glutamine, 100 U/mL
206 penicillin, 100 $\mu\text{g/mL}$ streptomycin) into 24-well flat-bottom plates and incubated for 12h at 37°C, in 5% CO₂. In
207 *in vitro* inhibition studies of Brd4 or MTF-1, the cells were pretreated with JQ1 (Sigma; 50 - 5000 ng/mL) or

208 APTO-253 (Medchemexpress; 1 - 4 $\mu\text{g}/\text{mL}$) for 6 h and incubated with 8-mix cytokines for an additional 24 h at
209 37°C, in 5% CO_2 .

210 Total RNAs were extracted with RNeasy Micro Kit (Qiagen) and were reverse-transcribed to cDNA with random
211 primers (Invitrogen), dNTP mixture (Takara), ribonuclease inhibitor (Promega) and SuperScript III (Invitrogen).
212 Quantitative real-time PCR (qRT-PCR) was performed using CFX Connect Real-Time PCR Detection System
213 (Bio-Rad) with QuantiTect SYBR Green PCR Kit (Qiagen). The primer pairs used in this study are shown in online
214 supplementary table 6. Relative expression was calculated based on the abundance of control *GAPDH*.

215

216 **Human IL-6 and CCL5 ELISA**

217 The concentration of IL-6 and CCL5 in supernatants of SFs was measured using the Human IL-6 Uncoated ELISA
218 Kit (Invitrogen) and Human CCL5/RANTES Quantikine ELISA Kit (R & D), respectively, according to the
219 manufacturer's instruction.

220

221 **Knockdown assay**

222 Purchased RASFs were used for knockdown assays. Cells (4×10^5 cells/target) were transfected with 300 nM
223 ON-TARGET plus siRNA targeting *MTF1*, *RUNX1*, *SNAI1* or *TCF4* (all from Dharmacon) using a Human Dermal
224 Fibroblast Nucleofector Kit (Lonza) according to the manufacturer's instructions. SiGENOME Non-Targeting
225 Control Pool (300 nM, Dharmacon) was used as a transfection control. Transfected cells (4×10^4 cells/well) were
226 seeded with DMEM (10% FBS, 100 $\mu\text{g}/\text{mL}$ L-glutamine, 100 U/mL penicillin, 100 $\mu\text{g}/\text{mL}$ streptomycin) into

227 24-well flat-bottom plates and incubated at 37°C, in 5% CO₂. After 6 h, cells were stimulated with 8-mix cytokines
228 for an additional 6 h. Total RNA was isolated using AllPrep DNA/RNA/miRNA Universal Kit. Libraries for RNA
229 sequencing were prepared using TruSeq Stranded mRNA Library Prep Kit. mRNA sequencing was carried out on
230 Illumina MiSeq (read length of 150 bp, paired end).

231

232 **CD40 stimulation assay**

233 Purchased RASFs (n = 3) were used in the CD40 stimulation assay. RASFs (2×10^4 cells/well) were seeded with
234 DMEM (10% FBS, 100 µg/mL L-glutamine, 100 U/mL penicillin, 100 µg/mL streptomycin) into 24-well
235 flat-bottom plates and incubated at 37°C, in 5% CO₂. After 12 h, cells were stimulated with 1 - 10 ng/mL CD40L
236 (ENZ) and 200 U/mL IFN-γ or 8-mix cytokines for an additional 24 h. RNA extraction, cDNA synthesis and
237 RT-PCR was performed as described above. Total RNA was isolated using AllPrep DNA/RNA/miRNA Universal
238 Kit. Libraries for RNA sequencing were prepared using TruSeq Stranded mRNA Library Prep Kit. The mRNA
239 sequencing was carried out on Illumina MiSeq (read length of 150 bp, paired end).

240

241 **Mice and induction of CIA**

242 DBA/1J male mice (6 weeks) were purchased from Japan SLC. To induce CIA, bovine type II collagen (CII;
243 Chondrex) was emulsified in equal volume of Complete Freund's Adjuvant (CFA; Chondrex). Mice were
244 intradermally injected with the emulsion (100 µL) containing 100 µg CII. Twenty-one days later, a secondary
245 injection was given at the same concentration of CII emulsified in Incomplete Freund's Adjuvant (IFA; Chondrex).

246 Mice were examined every day for clinical signs of arthritis after the first injection. The severity of arthritis was
247 assessed by qualitative clinical score determined as follows: 0 = normal paw; 1 =one toe inflamed and swollen; 2 =
248 >1 toe, but not entire paw inflamed and swollen, or mild swelling of entire paw; 3 = entire paw inflamed and
249 swollen; 4 = very inflamed and swollen or ankylosed paw. Each paw was scored individually and totaled them for
250 each mouse (a maximum of 16 points). All procedures were performed in accordance with National Institutes of
251 Health (NIH) Guide for the Care and Use of Laboratory Animals and approved by the ethics committee of the
252 University of Tokyo Institutional Animal Care and Use Committee.

253

254 **Treatment of CIA**

255 In the treatment experiment, following the onset of arthritis (clinical score >1), CIA mice were randomized into 2
256 groups and intravenously injected with either control (10% DMSO and 18% SBE- β -CD) or 15 mg/kg APTO-253 in
257 10% DMSO and 18% SBE- β -CD for twice per day for 2 consecutive days per week for 14 days. In the prophylaxis
258 experiment, on the same day as the second immunization, CIA mice were randomized into 2 groups and
259 intravenously injected with either control (10% DMSO and 18% SBE- β -CD) or 15 mg/kg APTO-253 in 10%
260 DMSO and 18% SBE- β -CD for twice per day for 2 consecutive days per week for 14 days.

261

262 **Histological assessment**

263 Mice were killed on day 15 after the start of treatment. Four paws were surgically removed and fixed in 4%
264 paraformaldehyde, decalcified in 20% EDTA and embedded in paraffin. Then, the sectioned tissues were stained

265 with haematoxylin and eosin (H&E) and Safranin O for histopathology. Synovial tissue thickening, mononuclear
266 cell infiltration, pannus invasion, and cartilage damage were graded. For synovial tissue thickening, scores were: 0,
267 no changes (thickness less than 0.7 mm at the patellar tendon); 1; mild changes (0.7-1.0 mm); 2, moderate changes
268 (1.0-2.0 mm); 3, severe changes (2.0 mm and more). For mononuclear cell infiltration, scores were: 0, no changes
269 (no infiltration); 1, mild changes (less than 150 cells in 0.07 μ m²); 2, moderate changes (150-300 cells); 3, severe
270 changes (300 cells or more). For pannus invasion, scores were: 0, no pannus; 1, mild changes (pannus invasion
271 within the cartilage); 2, moderate changes (pannus invasion into the cartilage/subchondral bone transition); 3,
272 severe changes (pannus invasion into the subchondral bone). For cartilage damage, scores were: 0, no destruction; 1,
273 minimal erosion limited to single spots; 2, slight to moderate erosion in a limited area; 3, more extended erosions; 4,
274 general destruction.

275

276 **Statistical analysis**

277 For *in vitro* analysis, statistical significance and analysis of variance (ANOVA) between indicated groups were
278 analyzed by R (ver 3.4.1). A comparison of more than 2 group means was analyzed by Tukey's multiple
279 comparison tests. A comparison of 2 group means was analyzed by paired t-test or Mann-Whitney U test.
280 Statistically significant differences were accepted at $P < 0.05$ for all tests. Data in the bar charts were expressed as
281 means \pm standard deviation (SD).

282 For large-scaled data analysis including differentially expressed gene analysis and eQTL analysis, multiple test
283 correction was performed with B-H method to obtain corrected q-values. For epigenome mark enrichment analysis

284 and transcriptome enrichment analysis with MAGMA, Bonferroni-corrected significance threshold was applied.

285

286 **Key resources information**

| REAGENT or RESOURCE | SOURCE | IDENTIFIER |
|---|--------------|---------------------------------|
| Antibodies | | |
| Rabbit polyclonal anti- H3K4me1 | Active Motif | Cat#39298; RRID: AB_2615075 |
| Rabbit polyclonal anti- H3K4me3 | Active Motif | Cat#39160; RRID: AB_2615077 |
| Rabbit polyclonal anti- H3K27ac | Active Motif | Cat#39134; RRID: AB_2561016 |
| Mouse monoclonal anti- CD3 (clone: UCHT1) | BioLegend | Cat#300419; RRID: AB_439780 |
| Mouse monoclonal anti- CD4 (clone: OKT4) | BioLegend | Cat#317433; RRID: AB_11150413 |
| Mouse monoclonal anti- CD8 (clone: RPA-T8) | BioLegend | Cat#301007; RRID: AB_314125 |
| Mouse monoclonal anti- CD14 (clone: M5E2) | BioLegend | Cat#301823; RRID: AB_893253 |
| Mouse monoclonal anti- CD19 (clone: HIB19) | BioLegend | Cat#302211; RRID: AB_314241 |
| Mouse monoclonal anti- CD56 (clone: HCD56) | BioLegend | Cat#318331; RRID: AB_10898118 |
| Mouse monoclonal anti- CD90 (Thy1) (clone: 5E10) | BioLegend | Cat#328107; RRID: AB_893438 |
| Biological Samples | | |
| Synovial specimen of human rheumatoid arthritis | This paper | N/A |
| Synovial specimen of human osteoarthritis | This paper | N/A |
| Peripheral blood of human rheumatoid arthritis | This paper | N/A |
| Peripheral blood of human osteoarthritis | This paper | N/A |
| Chemicals, Peptides and Recombinant Proteins | | |
| Human IFN- α 2A | HumanZyme | Cat#HZ-1066; GenPept: P01563 |
| Human IFN- γ | PeproTech | Cat#300-02; GenPept: P01579 |

| | | |
|--|----------------|--|
| Human TNF- α | PeproTech | Cat#300-01A; GenPept: P01375 |
| Human IL-1 β | PeproTech | Cat#200-01B; GenPept: P01584 |
| Human IL-6 | PeproTech | Cat#200-06; GenPept: P05231 |
| Human sIL-6R | PeproTech | Cat#200-06R; GenPept: P08887 |
| Human TGF- β 1 | R&D | Cat# 240-B-002/CF; GenPept: P01137 |
| Human IL-17 | PeproTech | Cat#200-17; GenPept: Q16552 |
| Human IL-18 | MBL | Cat#B001-5; GenPept: Q14116 |
| JQ1 | Sigma-Aldrich | Cat#SML1524; CAS: 1268524-70-4 |
| MEGACD40L | ENZ | Cat#ALX-522-110- C010 |
| APTO-253 | Medchemexpress | Cat#HY-16291; CAS: 916151-99-0 |
| Bovine Type II Collagen | Chondrex | Cat#20022 |
| Complete Freund's Adjuvant | Chondrex | Cat#7001 |
| Incomplete Freund's Adjuvant | Chondrex | Cat#7002 |
| Critical Commercial Assays | | |
| AllPrep DNA/RNA/miRNA Universal Kit | QIAGEN | Cat#80224 |
| RNeasy Micro Kit | QIAGEN | Cat#74004 |
| TruSeq Stranded mRNA Library Prep Kit | Illumina | Cat#RS-122-2101/2 102 |
| ChIP-IT High Sensitivity | Active Motif | Cat#53040 |
| ChIP-IT PBMC | Active Motif | Cat#53042 |
| TruSeq ChIP Library Preparation Kit | Illumina | Cat#IP-202-1012/1 024 |
| Nextera Mate Pair Sample Preparation Kit | Illumina | Cat#FC-132-1001 |
| Human Dermal Fibroblast Nucleofector Kit | Lonza | Cat#VPD1001 |
| Human IL-6 Uncoated ELISA Kit | Invitrogen | Cat#88-7066 |
| Human CCL5/RANTES Quantikine ELISA Kit | R&D | Cat#DRN00B |

| Deposited Data | | |
|--|-----------------------|---|
| Read counts data of RNA sequencing | This paper | NBDC: hum0207.v1.RNA.v1 |
| eQTL summary | This paper | NBDC: hum0207.v1.eQTL.v1 |
| Peaks data of CHIP sequencing | This paper | NBDC: hum0207.v1.ChIP.v1 |
| Chromatin loops data of Hi-C | This paper | NBDC: hum0207.v1.HiC.v1 |
| Experimental Models: Cell Lines | | |
| Synovial fibroblasts of human rheumatoid arthritis | Articular Engineering | Cat#CDD-H-2910-RA |
| Experimental Models: Organisms/Strains | | |
| Mouse: DBA/1J Jms Slc | SLC | RRID: MGI:5651994 |
| Oligonucleotides | | |
| ON-TARGET plus siRNA targeting MTF1 | Dharmacon | Cat#L-020078-00-0005 |
| ON-TARGET plus siRNA targeting RUNX1 | Dharmacon | Cat#L-003926-00-0005 |
| ON-TARGET plus siRNA targeting SNAI1 | Dharmacon | Cat#L-010847-01-0005 |
| ON-TARGET plus siRNA targeting TCF4 | Dharmacon | Cat#L-004594-00-0005 |
| SIGENOME Non-Targeting Control Pool #1 | Dharmacon | Cat#D-001206-13-05 |
| Software and Algorithms | | |
| R3.4.1 | R Core team, 2016 | https://www.R-project.org |
| Python 2.7 | Python Software | https://www.python.org/ |
| STAR (version 2.5.3) | Dobin et al, 2012 | https://github.com/alexdobin/STAR |

| | | |
|---------------------------|------------------------|---|
| HTSeq (version 0.6.0) | Anders et al, 2014 | https://github.com/simon-anders/htseq |
| RSEM (version 1.3.0) | Li et al, 2011 | https://github.com/deweylab/RSEM |
| RUVseq (version 1.10.0) | Risso et al, 2014 | https://github.com/drisso/RUVSeq |
| edgeR (version 3.18.1) | Robinson et al, 2010 | https://bioconductor.org/packages/release/bioc/html/edgeR.html |
| MAGMA (version 1.07) | de Leeuw C et al, 2015 | https://ctg.cncr.nl/software/magma |
| Bowtie2 (version 2.3.4.2) | Langmead et al, 2009 | https://github.com/BenLangmead/bowtie2 |
| MACS 2.0 (version 2.1.1) | Zhang et al, 2008 | https://github.com/tao-liu/MACS |
| ROSE | Whyte et al, 2013 | http://younglab.wi.mit.edu/super_enhancer_code.html |
| HOMER (version 4.9.1) | Heinz et al, 2010 | http://homer.ucsd.edu/homer/ |
| MotifDb (version 1.18.0) | Shannon et al, 2019 | http://bioconductor.org/packages/release/bioc/html/MotifDb.html |
| BWA (version 0.7.17) | Li et al, 2009 | https://github.com/lh3/bwa |
| JUICER (version 1.5) | Durand et al, 2016 | https://github.com/aidentlab/juicer |
| HiCCUPS | Rao et al, 2014 | https://github.com/aidentlab/juicer/wiki/HiCCUPS |
| PLINK (v1.90b4.4) | Purcell et al, 2007 | https://github.com/cchrchang/plink-ng/ |

| | | |
|----------------------------------|------------------------|---|
| SHAPEIT (v2.r904) | Delaneau et al, 2012 | https://mathgen.stats.ox.ac.uk/genetics_software/shapeit/shapeit.html |
| IMPUTE2 (version 2.3.2) | Howie et al, 2009 | https://mathgen.stats.ox.ac.uk/impute/impute_v2.html |
| SNPTEST (version 2.5.4) | Marchini et al, 2007 | https://mathgen.stats.ox.ac.uk/genetics_software/snptest/snptest.html |
| Meta-Tissue (version 0.5) | Sul et al, 2013 | http://genetics.cs.uccla.edu/metatissue/ |
| PEER (version 1.0) | Stegle et al, 2010 | https://github.com/PMBio/peer/wiki |
| QTLtools | Delaneau, 2017 | https://qtltools.github.io/qtltools/ |
| SNPSNAP | Pers et al, 2014 | https://data.broadinstitute.org/mpg/snp-snap/ |
| GSVA (version 1.24.2) | Hänzelmann et al, 2013 | https://bioconductor.org/packages/release/bioc/html/GSVA.html |
| BEDTools (version 2.26.0) | Quinlan et al, 2010 | https://github.com/arq5x/bedtools2 |
| MSigDB (version 7.1) | Liberzon et al, 2011 | https://www.gsea-msigdb.org/gsea/msigdb/index.jsp |
| clusterProfiler (version 3.16.1) | Yu et al, 2012 | https://bioconductor.org/packages/release/bioc/html/clusterProfiler.html |
| Other | | |
| Human CD14 MicroBeads | Miltenyi Biotec | Cat#130-050-201 |
| Mbo I | NEB | Cat#R0147S |
| Biotin-14-dATP | Invitrogen | Cat#19524016 |

| | | |
|---------------------------------------|------------|--------------|
| Dynabeads™ MyOne™ Streptavidin T1 | Invitrogen | Cat#65601 |
| SuperScript III Reverse Transcriptase | Invitrogen | Cat#18080093 |
| Random Primers | Invitrogen | Cat#48190011 |
| dNTP Mixture | Takara | Cat#4030 |
| RNasin® Plus Ribonuclease Inhibitor | Promega | Cat#N2611 |
| QuantiTect SYBR Green PCR Kit | QIAGEN | Cat#204143 |

287

288 **Online supplementary note 1. The estimated enrichment of SF populations revealed by single-cell RNA**

289 **sequencing analysis of freshly isolated SFs.**

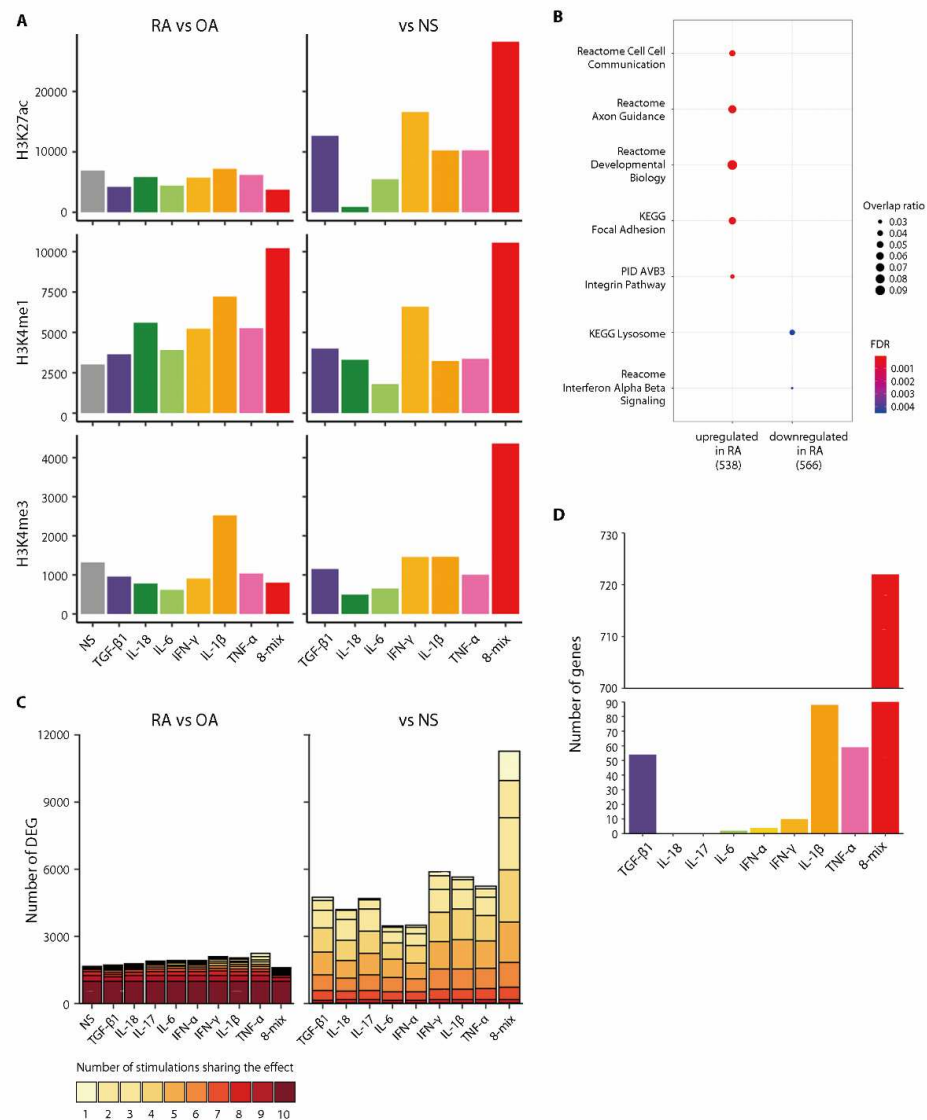
290 Fan Zhang *et al* reported three sublining subpopulations, namely CD34⁺ (F1), HLA-DRA^{hi} (F2) and DKK3⁺ (F3),
291 and one lining subpopulation (F4) based on single-cell RNA sequencing.[6] To elucidate the association between
292 transcriptional changes of activated SFs and those 4 fractions, we applied “top 20 marker genes for each single-cell
293 RNA sequencing cluster” for enrichment score calculation, and the population enrichment score of our stimulated
294 SFs was calculated using GSVA software.[7] F4 is the population most abundant in the lining of OA synovium, and
295 interestingly, the F4 score was higher in OASFs irrespective of the stimulation (online supplementary figure 11). In
296 contrast, F2 is the major IL-6 producer in the sublining, and the F2 score was strongly upregulated under IFN- γ ,
297 IFN- α , IL-6 or 8-mix stimulation and showed no difference between RA and OA. Accordingly, we surmised that
298 the F4 population was quantitatively stable between the diseases, although the F2 population might be inducible
299 under inflammation.

300

301 **Online supplementary note 2. Contribution of each cytokine to 8-mix condition.**

302 The epigenomic modifications in the 8-mix were deciphered into additive effects of 8 stimulations and non-additive
303 effects, which might be the consequence of cytokine synergy. The additive effect largely consisted of changes
304 induced by the combination of 3 or 4 kinds of cytokines including IL-1 β , IFN- α and/or IFN- γ (online
305 supplementary figure 12). A part of non-additive H3K27ac peaks formed distinct SEs (figure 5B), and some RA
306 risk loci including rs28411352 overlapped with those SEs.

307



308

309 **Online supplementary figure 1. Overview of transcriptomic and epigenomic signatures in RASFs under**
 310 **stimulatory conditions.**

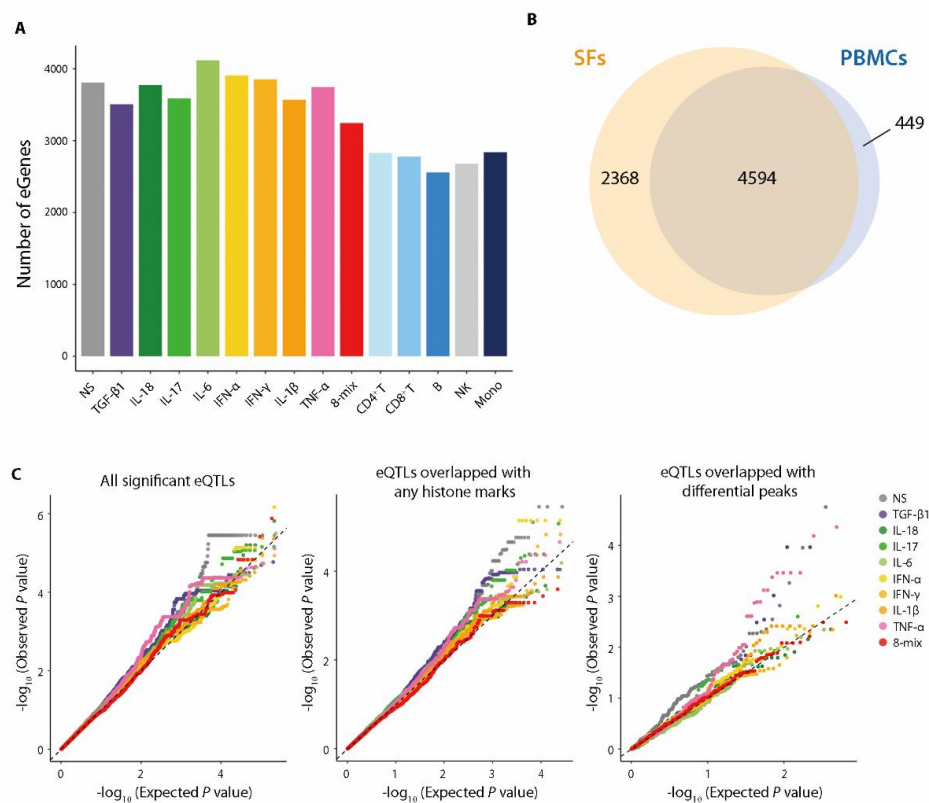
311 (A) The number of differential peaks from CHIP sequencing. Left, RA vs OA; Right, stimulated SFs vs

312 non-stimulated SFs. (B) Significantly enriched pathways for differentially expressed genes comparing RASFs and

313 OASFs under non-stimulated condition. **(C)** The number of differentially expressed genes from RNA sequencing.
314 Left, RA vs OA; Right, stimulated SFs vs non-stimulated SFs. Bar plots are colored by the number of stimulations
315 sharing the effects. Left, RA vs OA; Right, stimulated SFs vs non-stimulated SFs. **(D)** The number of genes for
316 which the response to stimulation were significantly different between RASFs and OASFs ($FDR < 0.05$). For each
317 stimulation, gene expression was analyzed with non-stimulated SFs, and disease-stimulation interaction term was
318 tested for significance.

319 SFs, synovial fibroblasts; RA, rheumatoid arthritis; OA, osteoarthritis; NS, non-stimulated; DEG, differentially
320 expressed genes.

321



322

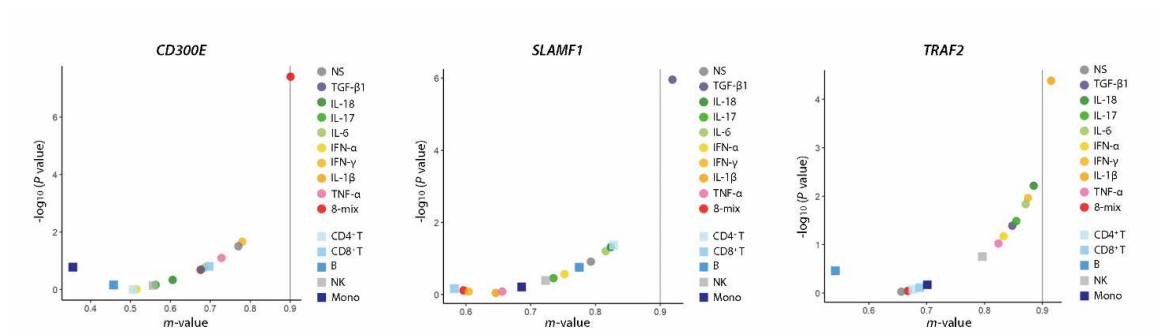
323 **Online supplementary figure 2. Summary of the results of cis-eQTL analysis in stimulated SFs and PBMCs**
 324 **from RA and OA patients.**

325 (A) The number of eGenes in stimulated SFs and PBMCs. (B) A Venn diagram representing the overlap of eGenes
 326 in SFs (in any condition) and PBMCs. (C) Distribution of disease-eQTL interaction P values compared to expected
 327 null distribution. When analyses were limited to eQTL variants overlapping with differential epigenome peaks
 328 between RA and OA (right panel), the interaction becomes more obvious compared to when analyses were
 329 performed with eQTL variants overlapping with any histone marks (middle) or all of the eQTL variants (left).

330 SFs, synovial fibroblasts; PBMC, peripheral blood mononuclear cell; RA, rheumatoid arthritis; OA, osteoarthritis;

331 NS, non-stimulated; eQTL, expression quantitative trait locus.

332



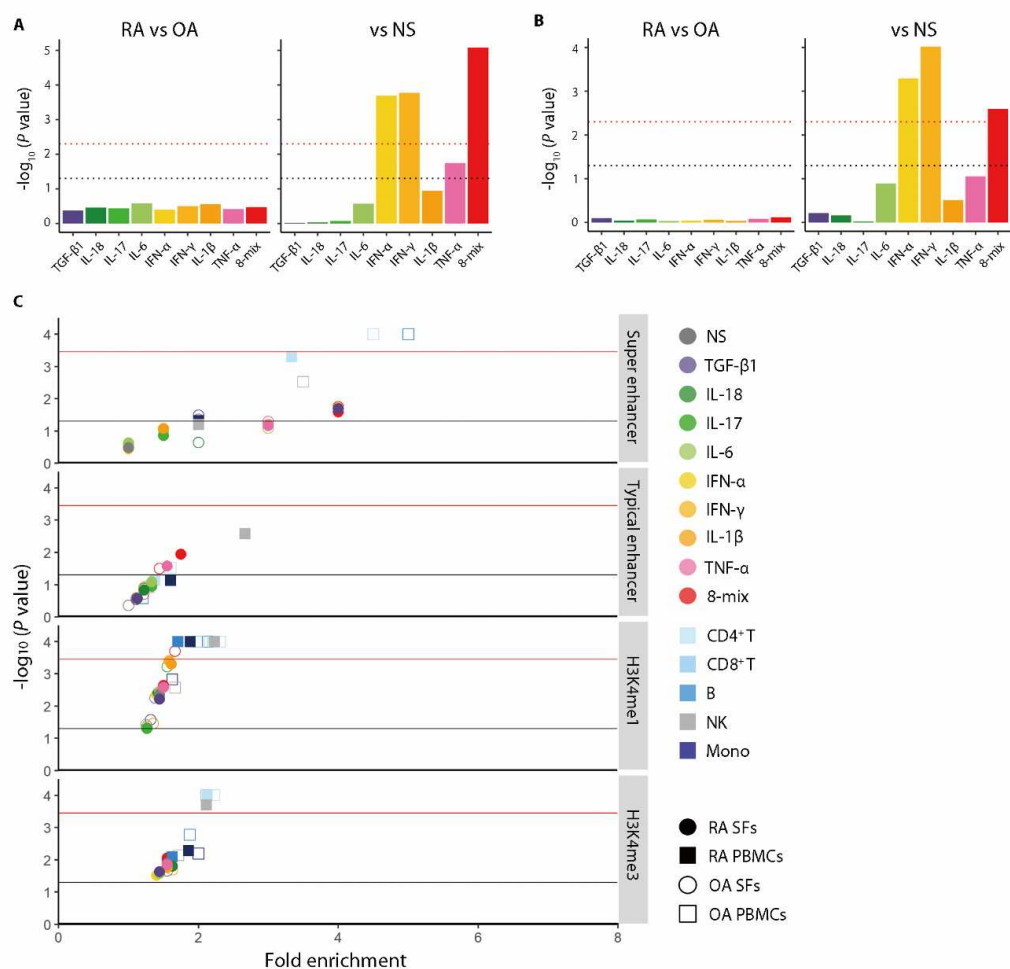
333

334 **Online supplementary figure 3. Representative examples of eQTL in stimulated SFs.**

335 (A to C) Examples of stimulation-specific eQTLs. A dot plot of cis-eQTL meta-analysis posterior probability

336 *m*-value and tissue-by-tissue analysis $-\log_{10} P$ value for rs8069701-*CD300E* (A), chr1:160179300-*SLAMF1* (B) and337 rs914744-*TRAF2* (C) are shown.

338 SFs, synovial fibroblasts; NS, non-stimulated; eQTL, expression quantitative trait locus.

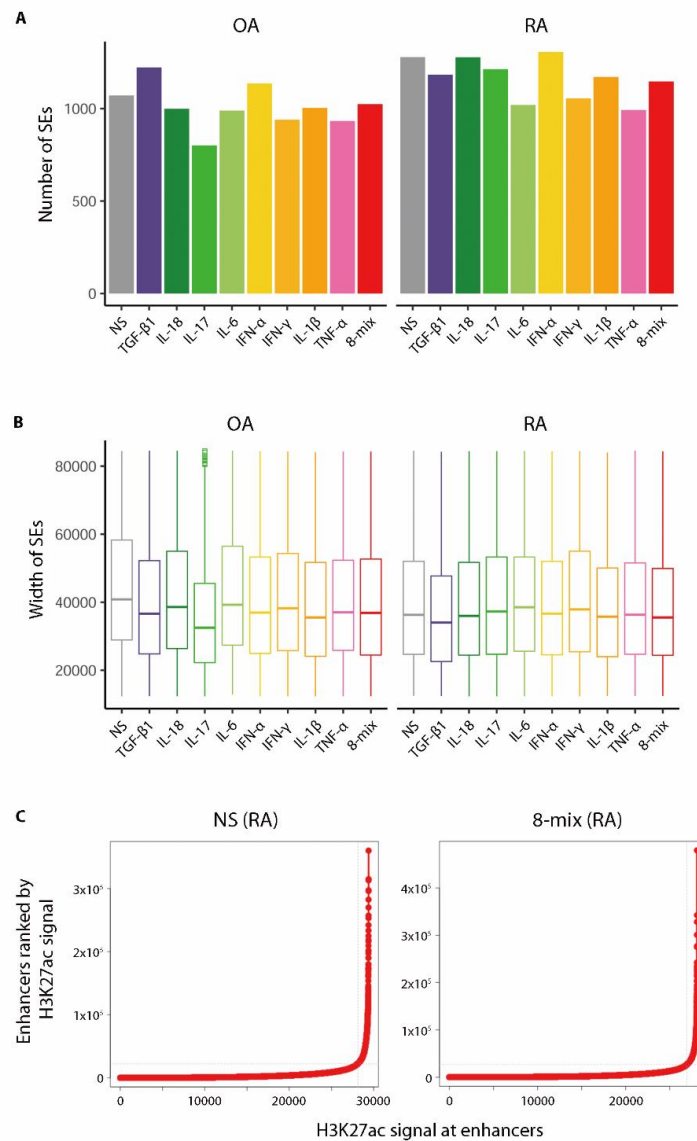


339

340 **Online supplementary figure 4. Polygenic association between differentially expressed genes and RA risk**341 **variants, and GWAS-super-enhancers enrichment analysis in Type 1 diabetes mellitus.**342 **(A, B)** Polygenic association analysis of differentially expressed genes with RA genetic risk using EUR GWAS **(A)**343 and EAS GWAS **(B)** data. Association *P* values were calculated with MAGMA. The red dotted lines and the black344 dotted lines are the cutoff for Bonferroni significance and *P* = 0.05, respectively. **(C)** Enrichment of type 1 diabetes

345 mellitus risk loci in transcriptional regulatory regions of stimulated SFs and PBMCs. Active enhancers were

346 classified into super-enhancers (SEs) and typical-enhancers (TEs) following standard ROSE algorithms. The red
347 solid lines and the black solid lines are the cutoff for Bonferroni significance and $P = 0.05$, respectively.
348 SFs, synovial fibroblasts; PBMC, peripheral blood mononuclear cell; RA, rheumatoid arthritis; OA, osteoarthritis;
349 NS, non-stimulated; SE, super enhancer; TE, typical enhancer; GWAS, genome-wide association study.
350



351

352 **Online supplementary figure 5. Comparison of the number and width of SEs in SFs among different**
 353 **stimulatory conditions.**

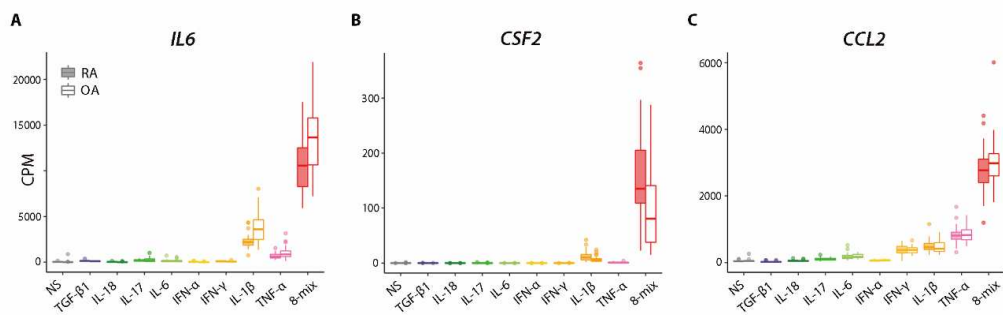
354 (A) The number of SEs of each stimulated SFs. (B) The width of SEs of each stimulated SFs. Boxes, interquartile

355 range; whiskers, distribution. (C) Distribution of SEs based on H3K27Ac signals and enhancer ranks in

356 non-stimulated (left) and 8-mix stimulated (right) RASFs.

357 SFs, synovial fibroblasts; RA, rheumatoid arthritis; OA, osteoarthritis; NS, non-stimulated; SE, super enhancer.

358



359

360 **Online supplementary figure 6. Synergistic effect of cytokines on epigenomic modifications and**

361 **inflammatory gene expression.**

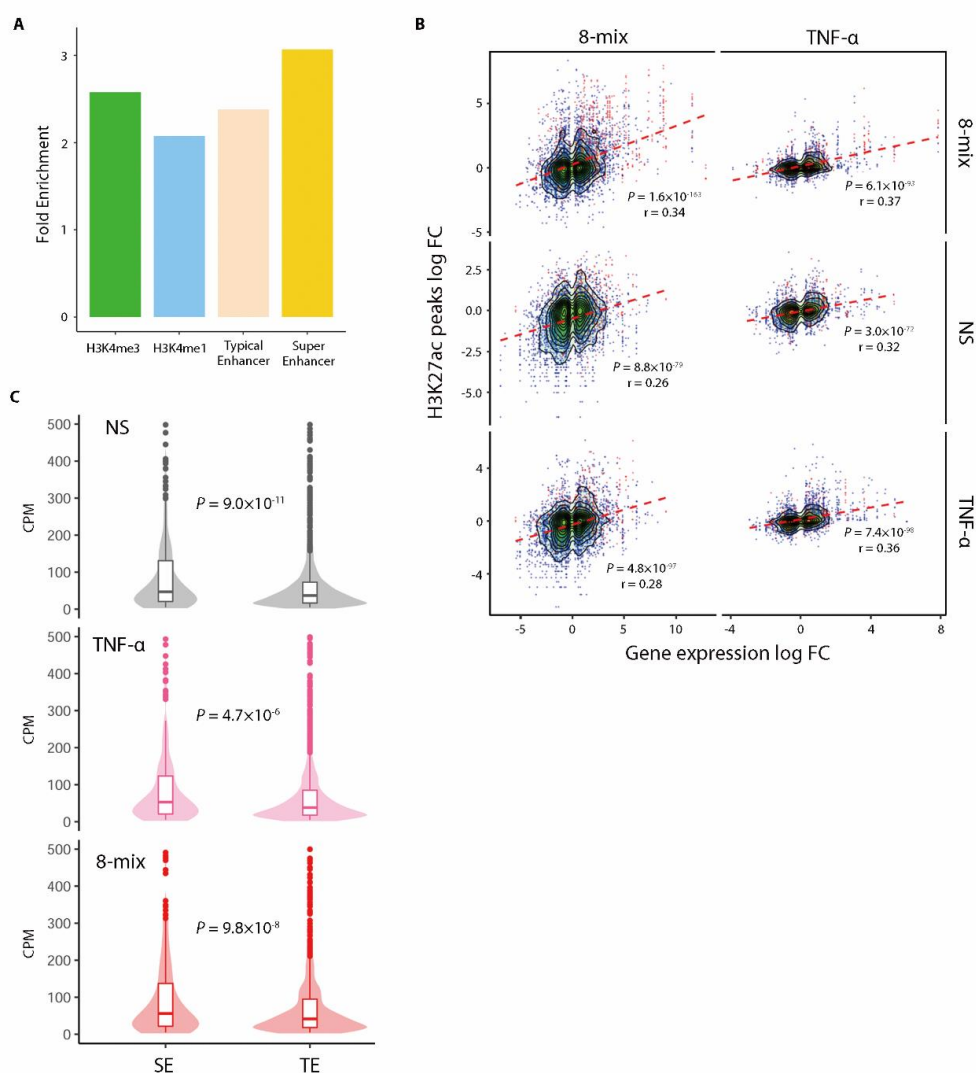
362 (A to C) Transcript abundances of representative RA pathogenic genes, *IL6* (A), *CSF2* (B) and *CCL2* (C) from

363 RNA sequencing data in stimulated SFs. Boxes, interquartile range; whiskers, distribution; dots, outliers.

364 SFs, synovial fibroblasts; RA, rheumatoid arthritis; OA, osteoarthritis; NS, non-stimulated; CPM, counts per

365 million.

366



367

368 **Online supplementary figure 7. The relevance among Hi-C loop, SEs and gene expression levels.**

369 (A) The enrichment of Hi-C loop anchors with epigenome status (H3K4me3 peaks, H3K4me1 peaks, TEs and SEs).

370 Fold change was calculated compared with randomly selected loci from the whole genome. (B) Comparison of

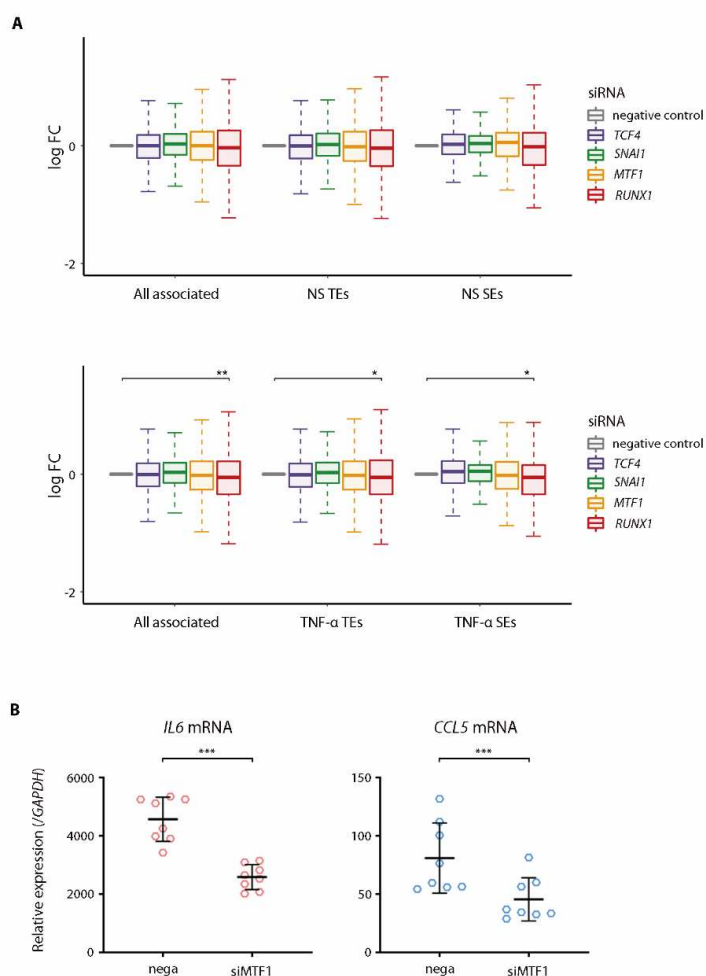
371 H3K27ac peak fluctuation and its associated gene expression fluctuation. Associated gene for each H3K27ac peak

372 was determined with Hi-C loops. Fold change between RA and OA samples are compared. In the left panel, genes

373 and H3K27ac peaks were connected with Hi-C loops in 8-mix stimulated SFs. In the right panel, genes and
374 H3K27ac peaks were connected with Hi-C loops in TNF- α stimulated SFs. Top, comparison in 8-mix stimulated
375 SF samples; middle, comparison in non-stimulated SF samples; bottom, comparison in TNF- α stimulated SF
376 samples. *P* values and ρ were calculated using Spearman's test. Red dot, SE-contacting genes; Blue dot,
377 TE-contacting genes. (C) Transcript abundances of TE or SE-contacting genes from RNA sequencing data for
378 stimulated SFs. Boxes, interquartile range; whiskers, distribution; dots, outliers; density plot, frequency. *P* values
379 were calculated with Student t test.

380 SFs, synovial fibroblasts; RA, rheumatoid arthritis; OA, osteoarthritis; NS, non-stimulated; SE, super enhancer; TE,
381 typical enhancer; CPM, counts per million.

382

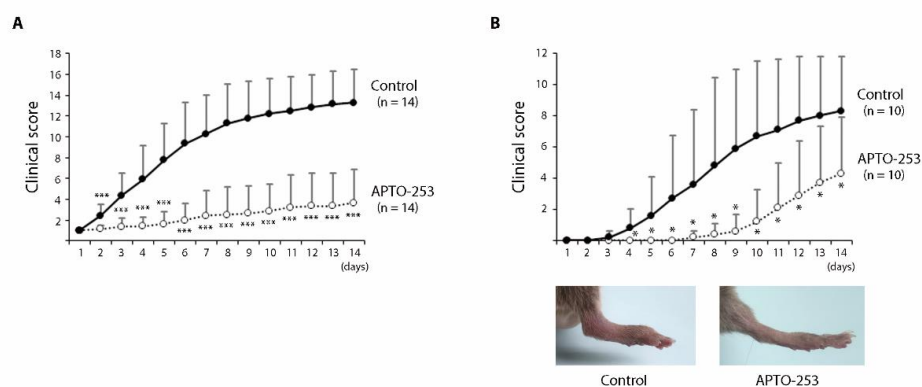


383

384 **Online supplementary figure 8. Transcription factors associated with SEs formation in 8-mix stimulated SFs.**385 (A) Expression of non-stimulation or TNF- α TE or SE-contacting genes in transcription factors (*TCF4*, *SNAI1*,386 *MTF1* and *RUNX1*) -depleted SFs relative to control SFs. Boxes, interquartile range; whiskers, distribution. *P*387 values were calculated using a paired t test ($*P < 0.05$, $**P < 0.01$). (B) Transcript abundances of *IL6* and *CCL5*388 from qRT-PCR data in *MTF1*-depleted SFs ($n = 8$). Horizontal crossbars, mean; error bars, SD. *P* values were389 calculated using a paired t test ($***P < 0.001$).

390 SFs, synovial fibroblasts; NS, non-stimulated; SE, super enhancer; TE, typical enhancer.

391



392

393 **Online supplementary figure 9. Preventive effect of APTO-253 on CIA model.**

394 (A) The replication of therapeutic effect of APTO-253 on CIA model (also see figure 8). Dots, mean; Error bars,

395 SD. *P* values were calculated using a Mann–Whitney U test (***, *P* < 0.001).

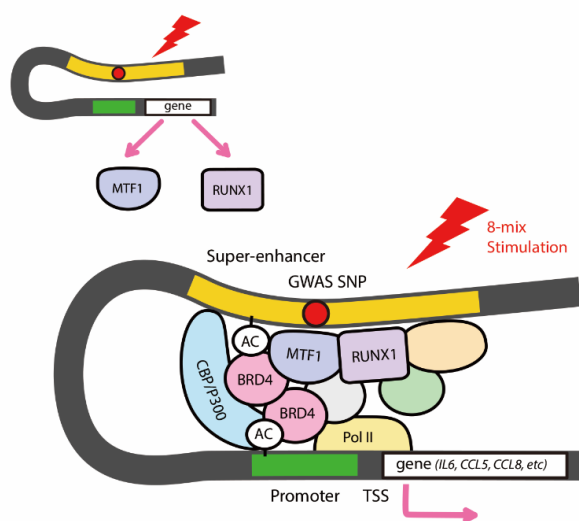
396 (B) On the same day as the second immunization, CIA mice were intravenously injected with either control or 15

397 mg/kg APTO-253 for twice per day for 2 consecutive days per week. Clinical scores in each group and

398 representative pictures of hind paw. Dots, mean; Error bars, SD. *P* values were calculated using a Mann–Whitney399 U test (*, *P* < 0.05).

400 CIA, collagen-inducer arthritis.

401

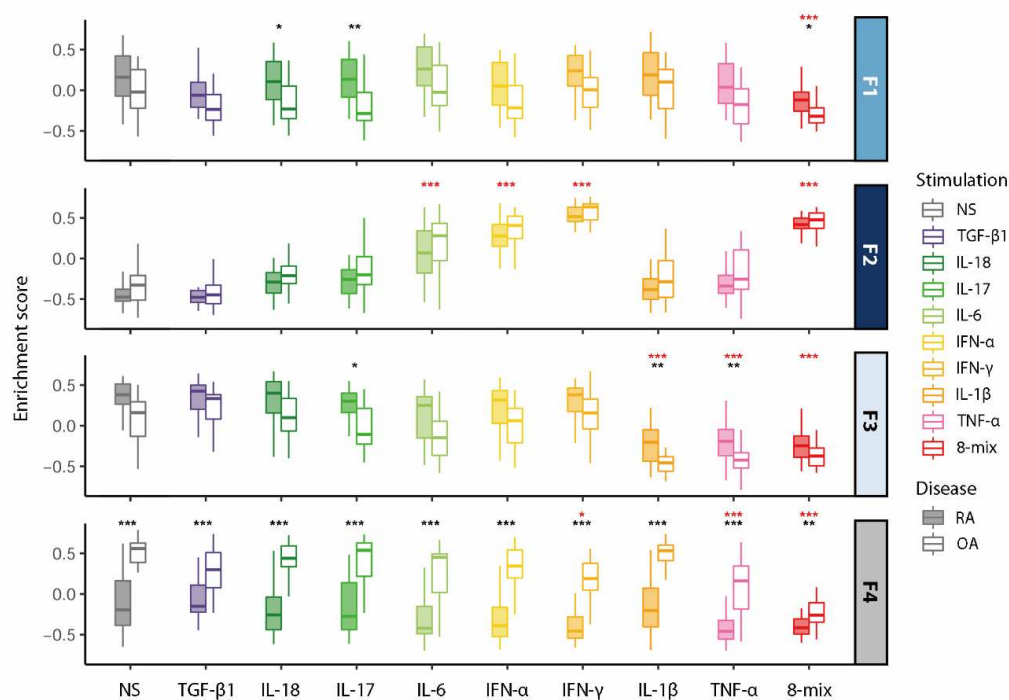


402

403 **Online supplementary figure 10. A Graphical summary of the present study.**

404 The authors conducted integrated analysis of stimulated SFs and demonstrated chromatin remodeling in the
405 presence of synergistic proinflammatory cytokines. The dynamic changes with super-enhancer formation are
406 associated with RA heritability. Transcription factors including MTF1 and RUNX1 could be crucial for
407 structural arrangement and the marked increase in the expression of pathogenic molecules from SFs.
408 SFs, synovial fibroblasts; RA, rheumatoid arthritis; TSS, transcriptional start site; GWAS, genome-wide
409 association study.

410



411

412 **Online supplementary figure 11. The estimated enrichment of SF populations revealed by single-cell RNA**
 413 **sequencing analysis of freshly isolated SFs.**

414 The population enrichment score of our stimulated SFs was calculated using GSVA software. Fan Zhang *et al*

415 reported three sublining subpopulations, namely CD34⁺ (F1), HLA-DRA^{hi} (F2) and DKK3⁺ (F3), and one lining

416 subpopulation (F4) based on single-cell RNA sequencing.[6]

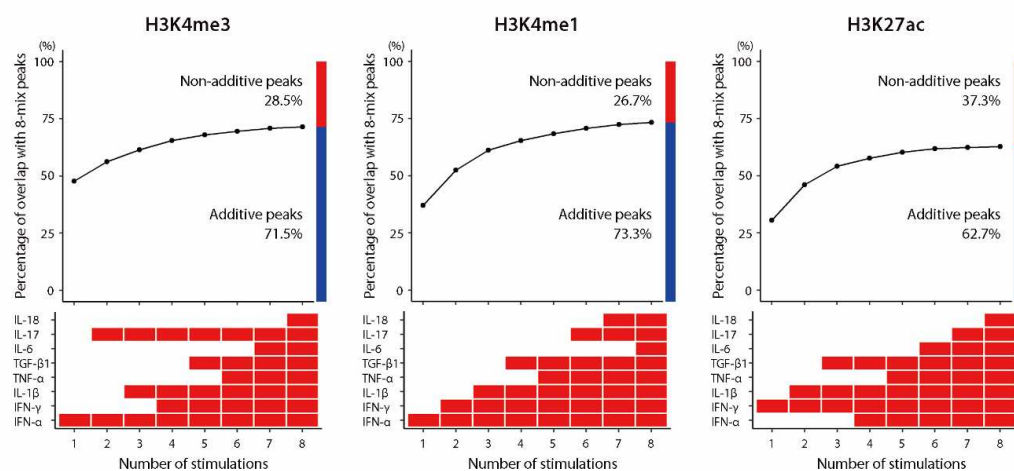
417 We applied “top 20 marker genes for each single-cell RNA sequencing cluster” for enrichment score calculation.

418 *P* values were calculated using a paired t test (**P* < 0.05, ***P* < 0.01, ****P* < 0.001, red, comparison between

419 stimulation and non-stimulation; black, comparison between RA and OA). Boxes, interquartile range; whiskers,

420 distribution.

421 RA, rheumatoid arthritis; OA, osteoarthritis; NS, non-stimulation; F1-4, Fraction 1-4.



422

423 **Online supplementary figure 12. Contribution of each cytokine to 8-mix condition.**

424 To decipher epigenomic modulations by the 8-mix into each cytokine, we compared the overlap of 8-mix-induced

425 peaks with the union of the individual cytokine simulation-induced peaks. All of the combinations of 1 - 8

426 cytokines were tested, and the combinations which accounted for the largest fraction of 8-mix-induced peaks are

427 plotted. The percentage of peak overlap between 8-mix-induced peaks and the best combination of individual

428 cytokine-induced peaks (upper plot) and the combination of cytokines (lower panel) are shown.

429

430 **Online supplementary table 1. Summary of differentially expressed genes (Separate file).**

431 Log fold changes and *P* values of comparisons between RA and OA or between stimulation and non-stimulation
432 are listed for all the analyzed genes. NA values indicates that the genes are not expressed highly enough for
433 comparisons.

434

435 **Online supplementary table 2. Disease-specific cis-eQTL signals (Separate file).**

436 List of the eQTLs whose effect sizes showed significant interactions with disease term. All the listed variants
437 overlap with differential epigenome peaks between RA and OA.

438

439 **Online supplementary table 3. Colocalization of RA GWAS and cis-eQTL signals (Separate file).**

440 The list of cis-eQTL top variants which are in LD with RA GWAS top-associated loci. Variant pairs with $R^2 > 0.6$
441 in EUR or EAS population in 1000G phase 3 data are listed. The RA GWAS top-associated SNP was downloaded
442 from the NHGRI-EBI GWAS Catalog.[8] EFO_0000685 was downloaded on 11/09/2018.

443 eQTL, expression quantitative trait locus; GWAS, lead variant in genome-wide association study; R^2 , r square
444 values between eQTL top variant and GWAS top-associated SNP in EUR or EAS population (the larger one is
445 written); method, eQTL analysis method for the indicated top eQTL variant; MT, meta-tissue analysis; TBT,
446 tissue-by-tissue analysis

447

448 **Online supplementary table 4. Summary of SE-contacted genes (Separate file).**

449 **Online supplementary table 5. Characteristics of patients for RNA sequencing.**

| | RA (n=30) | OA (n=30) |
|---------------------------------------|------------------|------------------|
| Age, years (range) | 70 (52-80) | 73 (54-88) |
| Female, n (%) | 26 (86.7) | 24 (80.0) |
| Serological markers | | |
| Rheumatoid factor-positive, n (%) | 25 (83.3) | 0 (0) |
| Anti-CCP autoantibody-positive, n (%) | 21 (70.0) | 0 (0) |
| Disease activity, n (%) | | |
| High (DAS-ESR >5.1) | 6 (20.0) | n/a |
| Moderate (DAS-ESR 3.2-5.1) | 20 (66.7) | n/a |
| Low/Remission (DS-ESR <3.2) | 4 (13.3) | n/a |
| Steinbrocker Stage, n (%) | | |
| I | 0 (0) | n/a |
| II | 3 (10.0) | n/a |
| III | 11 (36.7) | n/a |
| IV | 16 (53.3) | n/a |
| Steinbrocker Class, n (%) | | |
| I | 0 (0) | n/a |
| II | 17 (56.7) | n/a |
| III | 11 (36.7) | n/a |
| IV | 2 (6.7) | n/a |
| Treatment, n (%) | | |
| csDMARDs | | |
| MTX | 14 (46.7) | 0 (0) |
| BUC | 5 (16.7) | 0 (0) |
| IGU | 4 (13.3) | 0 (0) |
| SASP | 5 (16.7) | 0 (0) |
| TAC | 5 (16.7) | 0 (0) |
| Glucocorticoids | 21 (70.0) | 0 (0) |
| boDMARDs | | |
| TNFi | 6 (20.0) | 0 (0) |
| ABT | 2 (6.7) | 0 (0) |
| TCZ | 2 (6.7) | 0 (0) |

450

451

- 452 RA, rheumatoid arthritis; OA, osteoarthritis; csDMARDs, conventional synthetic disease-modifying antirheumatic
- 453 drugs; MTX, methotrexate; BUC, bucillamine; IGU, iguratimod; SASP, salazosulfapyridine; TAC, tacrolimus;
- 454 boDMARDs, biological originator disease-modifying antirheumatic drugs; TNFi, tumour necrosis factor inhibitors;
- 455 ABT, abatacept; TCZ, tocilizumab; n/a, not applicable.

456 **Online supplementary table 6. Sequences of primer pairs used in qRT-PCR.**

| Target | Sequence (Forward) | Sequence (Reverse) |
|--------------|----------------------------------|----------------------------------|
| <i>IL6</i> | 5'- GCCTTCGGTCCAGTTGCCTT -3' | 5'- AGTGCCTCTTTGCTGCTTTTAC -3' |
| <i>CCL5</i> | 5'- AGTGTGTGCCAACCCAGAGAAGAA -3' | 5'- TGTGGTAGAATCTGGGCCCTTCAA -3' |
| <i>MTF1</i> | 5'- GCCCCAGTAATGGCTGTGAG -3' | 5'- TCCTCTGATCCATTGTGTTGTGG -3' |
| <i>RUNX1</i> | 5'- TCCACTGCCTTTAACCCCTCA -3' | 5'- AGGTGAAATGGGCGTTGCT -3' |
| <i>SNAI1</i> | 5'- TATGCTGCCTTCCCAGGCTTG -3' | 5'- ATGTGCATCTTGAGGGCACCC -3' |
| <i>TCF4</i> | 5'- TCCAGGTTTGCCATCTTCAGT -3' | 5'- GCCTGGCGAGTCCCTATTG -3' |
| <i>GAPDH</i> | 5'- GAAGGTGAAGGTCGGAGTC -3' | 5'- GAAG ATGGTGATGGGATTTC -3' |

457

458

459 **Online supplementary references**

- 460 1 Aletaha D, Neogi T, Silman AJ, et al. 2010 Rheumatoid arthritis classification criteria: an American
461 College of Rheumatology/European League Against Rheumatism collaborative initiative. *Arthritis and rheumatism*
462 2010;62:2569-81.
- 463 2 GTEx Consortium. Human genomics. The Genotype-Tissue Expression (GTEx) pilot analysis:
464 multitissue gene regulation in humans. *Science (New York, NY)* 2015;348:648-60.
- 465 3 Okada Y, Wu D, Trynka G, et al. Genetics of rheumatoid arthritis contributes to biology and drug
466 discovery. *Nature* 2014;506:376-81.
- 467 4 Landt SG, Marinov GK, Kundaje A, et al. ChIP-seq guidelines and practices of the ENCODE and
468 modENCODE consortia. *Genome research* 2012;22:1813-31.
- 469 5 Rao SS, Huntley MH, Durand NC, et al. A 3D map of the human genome at kilobase resolution reveals
470 principles of chromatin looping. *Cell* 2014;159:1665-80.
- 471 6 Zhang F, Wei K, Slowikowski K, et al. Defining inflammatory cell states in rheumatoid arthritis joint
472 synovial tissues by integrating single-cell transcriptomics and mass cytometry. *Nature immunology*
473 2019;20:928-42.
- 474 7 Hanzelmann S, Castelo R, Guinney J. GSVA: gene set variation analysis for microarray and RNA-seq
475 data. *BMC bioinformatics* 2013;14:7.
- 476 8 Buniello A, MacArthur JAL, Cerezo M, et al. The NHGRI-EBI GWAS Catalog of published
477 genome-wide association studies, targeted arrays and summary statistics 2019. *Nucleic acids research*

478 2019;47:D1005-d12.

479